

APPLICATION OF NEURAL STRUCTURES IN WATER QUALITY MEASUREMENTS

O. Postolache¹, M.D. Pereira², P. Girão³, M. Cretu¹ and C. Fosalau¹

¹ Faculty of Electrical Engineering Iasi, B-dul D. Mangeron 53, Iasi 6600, Romania

² Escola Superior de Tecnologia, Instituto Politécnico de Setúbal, Portugal

³ Instituto Superior Tecnico, SETME, Av. Rovisco Pais 1049-001, Lisboa, Portugal

Abstract: The paper presents a theoretical and practical study related with the implementation of artificial intelligence for the enhancement of water quality measurement systems accuracy. The measurement parameters related to water quality (WQ), considered in the present work, are essentially the pH and the conductivity (C). The fusion of sensor information is performed using two different architectures of the Artificial Neural Networks. Those architectures are compared in terms of the implementation, complexity of associated digital signal processing and accuracy enhancement. An additional measure of temperature is used to offer details regarding the presence of micro-organisms in tested water and also to compensate the temperature influences on the pH and C measurements. The test environment is implemented by a virtual measurement system, which includes a hardware component based on a data acquisition board and a software component developed in LabVIEW graphical programming language.

Keywords: Water Quality Measurement, Neural Networks, Accuracy

1 INTRODUCTION

The water quality is an important problem that affects the environment and the quality of life. The measurement systems associated with the monitoring of the water quality (WQ) are usually multisensor systems (MS). The knowledge of each WQ parameter, such as the temperature (T), the pH, the conductivity (C), the salinity or the dissolved oxygen (DO), imposes an increase in the complexity of the multisensor system. For complex MS, the usage of intelligent processing structures is required in order to compensate external disturbance effects [1] and to implement the fusion of sensor information [2]. One of the most applied intelligent structures in compensation and sensor fusion is the Artificial Neural Network (ANN). In these conditions, taking into account the advances in the neural processing area [3][4], in the present work several ANN architectures are studied, simulated and implemented on a multisensor system that extracts and processes the T, pH and C information.

2 SENSOR AND INTERFACE

Electrochemical sensors are generically used for WQ measurements. In the present application a set of Orion [5] sensors for pH and C measurements is used. The temperature information is obtained using a Smartec SMT 160-30 [6] temperature sensor.

Referring to pH sensor, it is represented by a waterproof triode pH electrode, which includes an Ag/AgCl internal reference system. For a precise measurement, the sensor was calibrated using two calibrating buffers, one a pH 7 buffer, and the second pH=4 and pH=10, the interval of values expected for the samples in the present application. The voltage information delivered by pH sensor is applied to an amplifier circuit based on MAX406 integrated circuit. The U_{pH} voltage, obtained after amplification, is applied to an analogue input channel (AI1) of the data acquisition board (DAQ) included in the system.

The conductivity is measured using an Orion conductivity standard (Orion 011007) that provides a variation of the output resistance as a function of water conductivity. The conditioning circuit of the C cell delivers a D.C. voltage proportional to the measured conductivity.

Analysing the behaviour of the pH and C cells as a function of temperature, an important temperature dependence of the measurements was detected for the temperature range, $T=[20;80]^{\circ}\text{C}$, of the proposed measurement system. The conductivity measurement error (ϵ_C) increases up to 1.5% and the pH measurement error (ϵ_{pH}) increases up to 3%, for the previous temperature range. These results underlined the importance of the knowledge of the temperature, to compensate temperature drift errors of the others sensors [1]. At the same time, the temperature information can be used as a reference for the measurement of other quality parameters in the water, such as the level of micro-organisms.

The temperature on the pH and C sensors level is measured with two smart temperature sensors (Smartec 160-30) that are positioned closely to pH and C sensors, as represented in Figure 1.

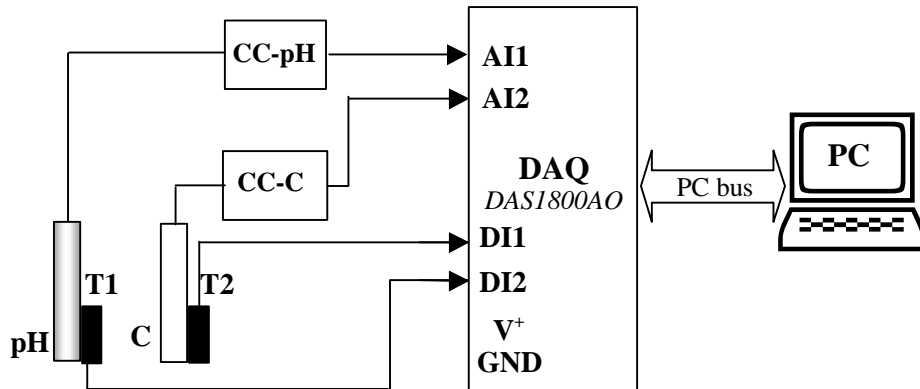


Figure 1. Hardware block diagram of the water quality measurement system (CC- conditioning circuit, DAQ- data acquisition board, PC- personal computer, T- tempetaure sensor, pH- pH sensor, C- conductivity sensor, AI- analogue input, DI- digital input).

The output signal from the temperature sensor is a duty-cycle-modulated (DC) square-wave voltage, which is linearly related to the temperature:

$$\text{DC} = 0.31924 + 0.00472 \times T(^{\circ}\text{C}) \quad (1)$$

Compared with others resistive sensor elements, such as thermistors, that are commonly used to extract the temperature information, this type of temperature sensors offers a number of advantages such as immunity to the resistance of the connection wires and insensitivity to electromagnetic interferences.

The signals of the T1 and T2 sensors are acquired using the digital inputs of a Keithley DAS1800AO DAQ [7]. This board includes a timer/counter block 82C54 with three 16-bit counters and the calculation of the DC value is performed by a software DC module. Signals from other sensors (pH, C) are applied to the analogue inputs of the board, AI1 and AI2.

As main characteristics of the DAQ used as interface between the transducers and PC, it can be referred the maximum sampling rate of 333 KS/s, 12 bit resolution and $\pm 100\text{mV}$, $\pm 1\text{V}$, $\pm 10\text{V}$, bipolar input voltage ranges.

3 ACQUISITION AND PROCESSING STRUCTURES

To extract the information regarding the WQ, a software component is associated with the hardware presented above. As main parts of the software it can be mentioned: the acquisition control, the duty-cycle (DC) calculation and the neural processing of pH, C and T information.

3.1 DC calculation

Due to the temperature gradient on the water volume, the WQ measurement system presented above includes two temperature sensors. The DC1 and DC2 values associated with each T sensor are calculated on the DC software modules developed in LabVIEW [8]. The main LabVIEW elements of these

modules are the Measure Pulse Width and Period subVI's. The calculation of DC is obtained by using the DAS1800 counter facilities for period and pulse width measurement of the signals generated by the temperature transducer. Finally the DC value is obtained and converted into temperature using the SMARTEC specifications. To minimise measurement errors, an average of 10 DC values is calculated and this average, together with (1), are used to express the temperature information. The DC1 and DC2 values are also directly used as inputs of the neural processing structures that extract the pH and C information compensated from temperature drift errors.

3.2 Neural processing structures

In the present work the numerical linearisation and the temperature compensation of the pH and C transducers are based on neural processing structures. The neural processing structures considered are associated with two different solutions. The first solution (Fig.2.a.) includes a modular neural network, Radial Basis Function (RBF-NN) [9] type. Thus the C information is extracted using the RBF-NN_C and the pH is extracted using RBF-NN_{pH}. The RBF-NNs are multi-input single-output (MISO) structures with the inputs being supplied by the duty cycle value (DC1 or DC2) and correspondent U_C and U_{pH} signals.

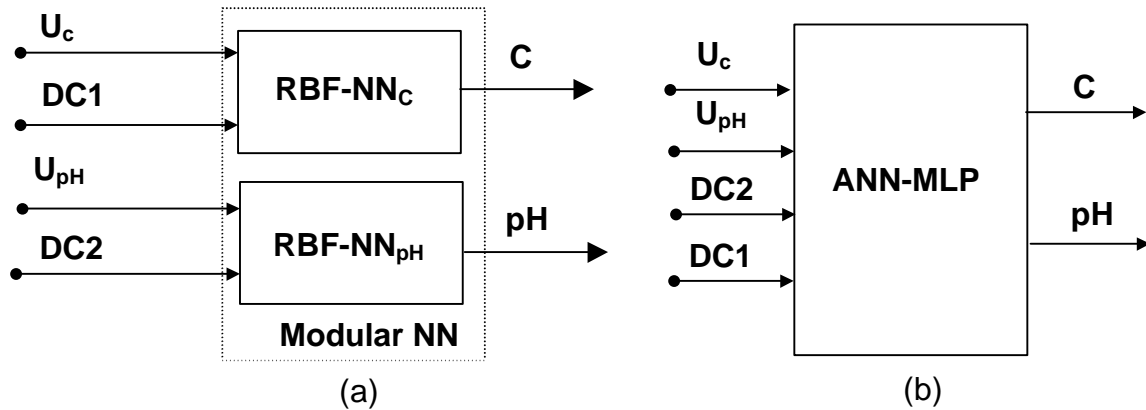


Figure 2. Block diagrams of the neural processing structures for C and pH information: (a) solution based on 2 radial basis function neural networks with single output; (b) solution based on a single multilayer perceptron neural network with 2 outputs.

Relating to the RBF-NN architecture, the hidden layer includes N_{hidden} gaussian neurons characterised by a Gauss function (Φ), defined by:

$$\Phi(r) = e^{-r^2 \cdot w^2}, \quad w > 0, \quad r \geq 0 \quad (2)$$

The neuron coordinates and weights are established using the training sets associated with the RBF-NN_C and RBF-NN_{pH} and the Kohonen algorithm implemented with the solverb MatLab function [10]. As stop algorithm condition it is used a predefined value of the sum squared error (SSE_{imposed}). The architectures are established in accordance with the required RBF-NN_i performances. In the present application, a value of $SSE_{\text{imposed}}=2E-4$ requires the utilisation a number of hidden neurons in the interval $N_{\text{hidden/RBF}}=[45;75]$. Each RBF-NN includes an output layer neurone that adds the hidden layer outputs values giving the RBFNN global response.

The second solution (Fig.2.b.) considered to extract the C and pH information is based on Multilayer Perceptron (MLP) architecture. In this case, the architecture includes a hidden layer with a number of neurons in the interval $N_{\text{hidden/MLP}} = [95;120]$, with tansigmoid activation functions. For each neuron, the weights and biases are established using the Levenberg-Marquardt algorithm starting from experimentally training sets. The stop algorithm condition used for this neural processing structure is also $SSE_{\text{imposed}}=2E-4$. Referring to input-output, the ANN-MLP includes 4 inputs associated to U_C, U_{pH}, DC1 and DC2 and two outputs corresponding to C and pH temperature compensated values.

In what concerns the establishment of the neural network training sets, these are obtained using several samples with the pH included in interval, $I_{pH}=[1;13]$, and the conductivity included in the interval, $I_C=[1;250][\mu S/cm]$. As was referred before, the temperature causes a major disturbance in C and pH measurements. For this reason, the calibration phase of the tested system is setup for different values of water temperature, included in the interval, $I_T=[0;100]^\circ C$.

4 RESULTS AND DISCUSSION

Considering the hardware and software components of the system, two different neural processing structures are evaluated and their results are compared in terms of accuracy and number of neurons required for each structure. Considering the tested water at several temperatures, a set of U_{pH} , U_C together with temperature values for each pH and C sensor was collected. The compensation of the temperature effect is based on RBF- NN_C , RBF- NN_{pH} and ANN-MLP using DC1 and DC2, calculated for the signals delivered by T1 and T2 as temperature sensors (DC=[41.2%; 79.1%]). The dimension of the matrixes for the elements of the modular neural processing are $dim(InC)=2 \times 35$, $dim(InpH)=2 \times 35$, $dim(OutC)=1 \times 35$ and $dim(OutpH)=1 \times 35$, where In and Out represent the input and output matrix for RBF- NN_C and RBF- NN_{pH} training. For experimental establishment of the training set, a study concerning the dependence number of RBF- NN_{pH} hidden neurons and RBF- NN_C versus the training stop condition $SSE_{imposed}=[1E-2;1E-7]$ was performed. The results for RBF- NN_{pH} are presented in the Figure 3.

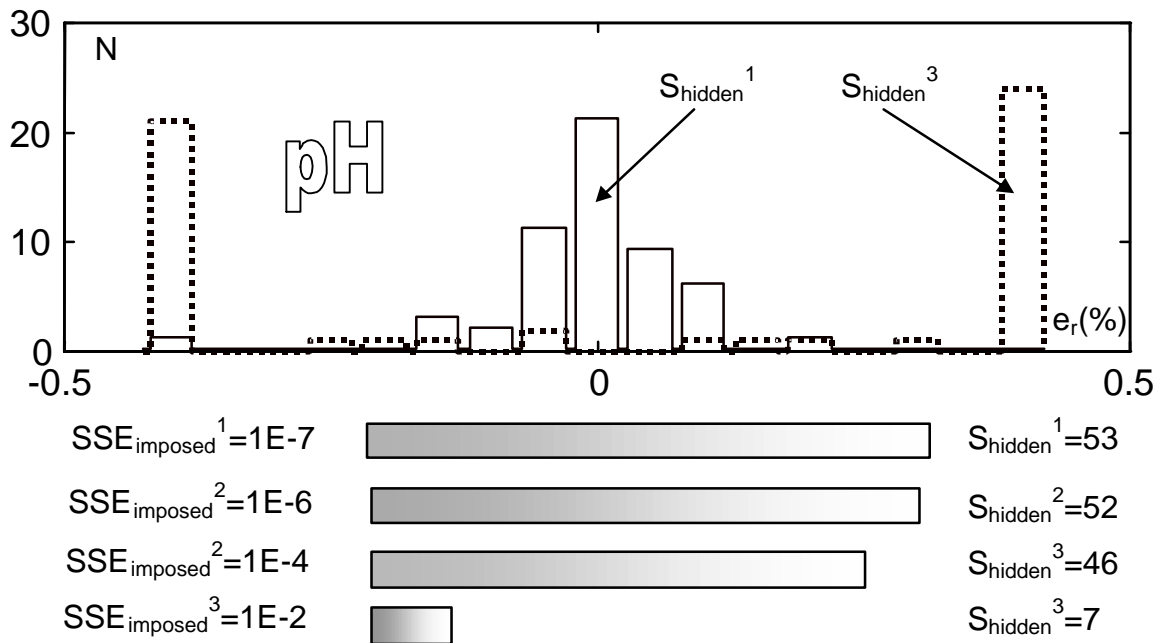


Figure 3. Histogram of $e_r(\%)$ and S_{hidden} dependence on $SSE_{imposed}$. N is the number of pH values having an e_r in the interval $e_{r1} \pm 0.025$. Total values of N: 54.

Analyzing the above presented figure, one can observe that the relative error, e_r , of the $pH=pH(U_{pH}, T2)$ dependence is lower than 0.1% for an RBF- NN_{pH} with 53 hidden neurons. The decreasing of the number of hidden neurons to S_{hidden}^3 conducts to a strong modification of e_r , the majority of errors for the $[U_{pH}, T2]$ test pairs being placed around 0.4%. The design of RBF- NN_C based on the training set conducts to a neural network that includes a reduced number of neurons for an imposed SSE. Thus, for $SSE_{imposed}=1E-7$, the number of hidden neurons is 7 but the $max(e_r)$ is about 10% which imposes the decrease of the RBF- NN_C stop condition to $SSE_{imposed}=1E-10$. After a new training for 22 hidden neurons, $SSE_{imposed}=1E-7$ is realized with e_r less than 0.5%. These results express that the RBF- NN_C will be materialized with a higher number of neurons in comparison to RBF- NN_{pH} , conducting to an increase of computation time.

Considering the same experimental training set, the design of the ANN-MLP was processed. In this case, the dimension of the input training matrix $dim(InMLP)$ is 4×35 the output training matrix being

$\dim(\text{OutMLP})=2 \times 35$. The number of hidden neurons is first considered to be 46 to compare the results with the RBF-NN case. Imposing $\text{SSE}_{\text{imposed}}=1\text{E}-4$, the number of epoch for obtaining an $\text{SSE} < \text{SSE}_{\text{imposed}}$ of the ANN-MLP training phase is 4. The e_r is calculated for C and pH situation using a test set. The distribution of the modeling relative error for C and pH case is expressed in Figure 4. Its components e_r^{C} and e_r^{pH} express the ANN capability to extract the C and pH information using the test values for U_{C} , DC2, U_{pH} , DC2. The network training was performed for the worst experimental simulated situation when $T1 \neq T2$.

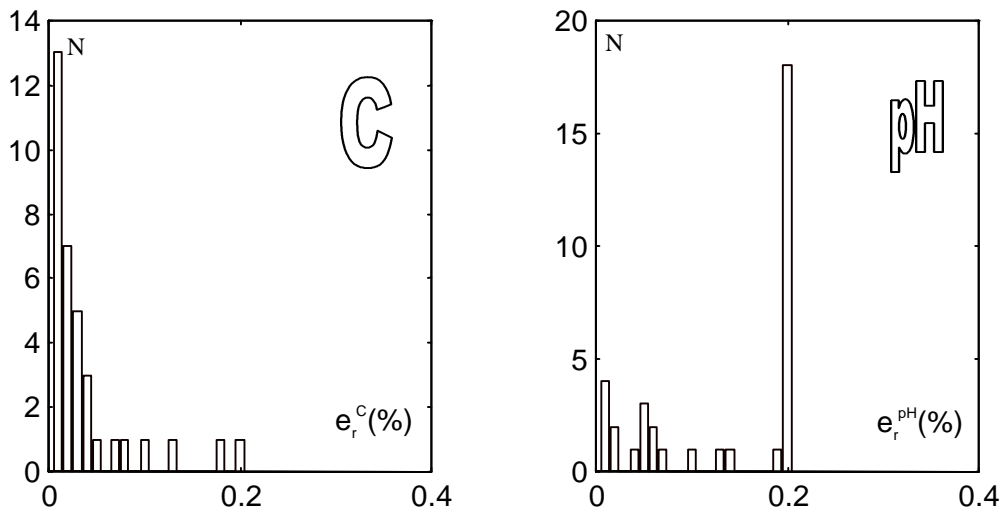


Figure 4. Histograms of The ANN-MLP modeling relative error components e_r^{C} and e_r^{pH} . Total number of N values in each histogram: 35.

Referring to the e_r^i distributions, it can be underlined that the C information is extracted with high accuracy for the entire temperature range. The extraction of the pH information is less accurate and it required a novel designing of ANN-MLP. Imposing $\text{SSE}=1\text{E}-7$ and 53 neurons, the results for the e_r^{C} and e_r^{pH} distributions are nearer, the majority of the values of e_r being distributed in the 0-0.1% zone. The training time increases in this case by three times.

Comparing the results for the RBF-NN and ANN-MLP applications, one can notice that ANN-MLP is characterized by a higher capacity to combine the information for the different sources (C, pH and T in the present case), the architecture requiring a higher number of neurons for the same accuracy. The RBF-NNs works better in modular application as was presented in the work.

5 CONCLUSIONS

Two neural processing structures to estimate the values of the conductivity and pH that measured by water probes solution in the presence of temperature as a disturbance factor has been. A comparison between the proposed neural structures, multiple inputs modular RBF-NN and multiple inputs – multiple outputs ANN-MLP, shows that the MLP is more adequate for application in multisensor automated measuring systems designed for WQ evaluation. The RBF-NN is characterized by better results as elements of the modular neural processing structure. According to these conclusions, future work will be focused on the implementation of RBF-NN modular structures using digital signal processors in multisensor WQ measuring systems.

REFERENCES

- [1] J.M. Dias Pereira, O. Postolache, P.M.B. Girão, "A Temperature-Compensated System for Magnetic Field Measurements Based on Artificial Neural Networks", *IEEE Transaction on Instrumentation and Measurement*, vol. 47, No.2. April, 1998, pp. 494-498.
- [2] O. Postolache, H. Ramos, P. Girao, J.Pereira and M.Cretu, "The multisensor ANN fusion method for accurate displacement measurement", *Buletinul IPI, Tom XLV,5A*, 1999, pp.364-369.

XVI IMEKO World Congress

Measurement - Supports Science - Improves Technology - Protects Environment ... and Provides Employment - Now and in the Future
Vienna, AUSTRIA, 2000, September 25-28

- [3] H. Kang, Q. Yang, C. Butler, "Modeling and Measurement Accuracy Enhancement of Flue Gas Flow Using Neural Networks", *IEEE Transaction on Instrumentation and Measurement*, vol. 47, No.5. October, 1998, pp.1379-1384.
- [4] A. Bernieri, "A Neural Network Approach for Identification and Fault Diagnosis on Dynamic Systems", *IEEE Transactions on Instrumentation and Measurement*, 1994, vol.43, No.6, pp.867-873.
- [5] Orion, Sensing the future – 1998 Laboratory Products and Electrochemistry Handbook, 1998.
- [6] Smartec., Specification sheet SMT 160-30, Breda, Netherlands, 1991.
- [7] Keithley Metrabyte, "DAS1800AO Series – LabVIEW VI Driver", 1994.
- [8] G.W. Johnson, "LabVIEW Graphical Programming – Practical Application in Instrumentation and Control", MacGraw Hill, New York, 1994.
- [9] V. Ferrari, A. Flammini, P. Maffezzoni, "Application of Neural Algorithms Based on Radial Basis Functions to Sensor Data Processing", *Proc. of IMEKO World Congress*, 1997, pp. 34-39.
- [10] K. Kemuth, "Neural Network Toolbox for Use with Matlab – User's Guide", The MathWorks Inc., September, 1993.

AUTHORS: O. POSTOLACHE, M.D. PEREIRA, M. CRETU and C. FOSALAU, Departamento de Sistemas e Informática, Escola Superior de Tecnologia, Instituto Politécnico de Setúbal, Rua do Vale de Chaves, Estefanilha, 2910 Setúbal, Portugal
Phone 351 265 790000, Fax 351 265 721869, E-mail: joseper@est.ips.pt